

Multi-wave mixing in the high harmonic regime: monitoring electronic dynamics: supplement

SHICHENG JIANG,¹  MARKUS KOWALEWSKI,² AND KONSTANTIN E. DORFMAN^{1,*} 

¹State Key Laboratory of Precision Spectroscopy, East China Normal University, Shanghai 200062, China

²Department of Physics, University of Stockholm, AlbaNova University Centre 106 91 Stockholm, Sweden

*dorfman@lps.ecnu.edu.cn

This supplement published with The Optical Society on 1 February 2021 by The Authors under the terms of the [Creative Commons Attribution 4.0 License](https://creativecommons.org/licenses/by/4.0/) in the format provided by the authors and unedited. Further distribution of this work must maintain attribution to the author(s) and the published article's title, journal citation, and DOI.

Supplement DOI: <https://doi.org/10.6084/m9.figshare.13603643>

Parent Article DOI: <https://doi.org/10.1364/OE.414619>

Multi-wave mixing in high harmonic regime: monitoring electronic dynamics: supplemental document

Ab-initio simulation

The coumarin molecule has been computed with at the sa-CASSCF(14/11)/6-31G* level of theory with the program package Molpro¹, including 11 electronic states. The coumarin ion has been calculated at a comparable level of theory sa-CASSCF(13/11)/6-31G* for 8 electronic states. The Dyson orbitals were calculated with program package OpenMolcas². The transition dipole moments from the neutral to the ion were calculated using a plane wave approximation for the unbound electron with momentum \mathbf{p} :

$$\mu_{mn}^{r_x}(\mathbf{p}) = \langle \phi_{mn}^D | r_x | e^{i\mathbf{p}\cdot\mathbf{r}} \rangle \quad (\text{S1})$$

where ϕ_{mn}^D is the Dyson orbital connecting state m of the neutral molecule with state n of the ion and r_x is the dipole operator for Cartesian component x .

Supplementary Discussion

we neglect the transition matrix elements between bound states for three reasons:

1) Usually the excitation without ionization and recombination won't generate obvious coherence between excited states separated broadly [see Fig. (2) in supplementary reference [3]].

2) We think that considering direct transition between bound states is equivalent to adding a constant term into the effective dipole in Eq. (5). Indeed, our method is applicable for well separated pulses (impulsive limit) and thus, the dynamics during the pulse can be neglected. Instead, we put more emphasis on the coherence oscillations, dephasing and population decay

during the interpulse delay, which is a typical focus of the time-resolved spectroscopies. Thus, even if the coupling between bound states is included, there won't be a significant impact on the Fourier transform of the time-domain signal.

(3) While the laser intensity we used is strong, the central frequency is far from electronic resonance. Thus, the excitation probability through perturbative process is very small. The Supplementary Figure 1 illustrates the signal obtained by Fourier transformation of time-delay dependent wave-mixing signal (3,1).

Polarization obtained from the channel of ionization-recombination can be written as

$$\begin{aligned}
P^{(1)}(\mathbf{k}_s=3\mathbf{k}_1+\mathbf{k}_2, \omega_s=3\omega_1+\omega_2, t) \\
= i \int_0^\infty dt_1 \left[\sum_m W_{gm}^{H,p_2}(q_2=1, t) W_{mg}^{H,p_1}(q_1=2, t-t_1) f_1(t-t_1) e^{-i3\omega_1 t_1 + i(\epsilon_m - \epsilon_g - i\gamma_{bc})t_1} \right]
\end{aligned}
\tag{S2}$$

On the other hand, the polarization from perturbative transition is given by

$$\begin{aligned}
P^{(3)}(\mathbf{k}_s=3\mathbf{k}_1+\mathbf{k}_2, \omega_s=3\omega_1+\omega_2, t) = \\
\int_0^\infty dt_3 \int_0^\infty dt_2 \int_0^\infty dt_1 S^{(3)}(t_3, t_2, t_1) f_1(t-t_3) f_1(t-t_3-t_2) f_1(t-t_3-t_2-t_1) e^{-i\omega(t_1+t_2+t_3) - i\omega(t_3+t_2) - i\omega t_3}
\end{aligned}
\tag{S3}$$

where

$$\begin{aligned}
S^{(3)}(t_3, t_2, t_1) &= i^3 \theta(t_1) \theta(t_2) \theta(t_3) \sum_{\alpha=1}^4 [R_\alpha(t, t_1, t_2, t_3) - R_\alpha^*(t, t_1, t_2, t_3)] \\
R_1(t, t_1, t_2, t_3) &= \langle \mu^b(t_1) \mu^b(t_1+t_2) \eta^{H,p_2}(t, t_1+t_2+t_3) \mu^b(0) \rangle \\
R_2(t, t_1, t_2, t_3) &= \langle \mu^b(0) \mu^b(t_1+t_2) \eta^{H,p_2}(t, t_1+t_2+t_3) \mu^b(t_1) \rangle \\
R_3(t, t_1, t_2, t_3) &= \langle \mu^b(0) \mu^b(t_1) \eta^{H,p_2}(t, t_1+t_2+t_3) \mu^b(t_1+t_2) \rangle \\
R_4(t, t_1, t_2, t_3) &= \langle \eta^{H,p_2}(t, t_1+t_2+t_3) \mu^b(t_1+t_2) \mu^b(t_1) \mu^b(0) \rangle
\end{aligned}$$

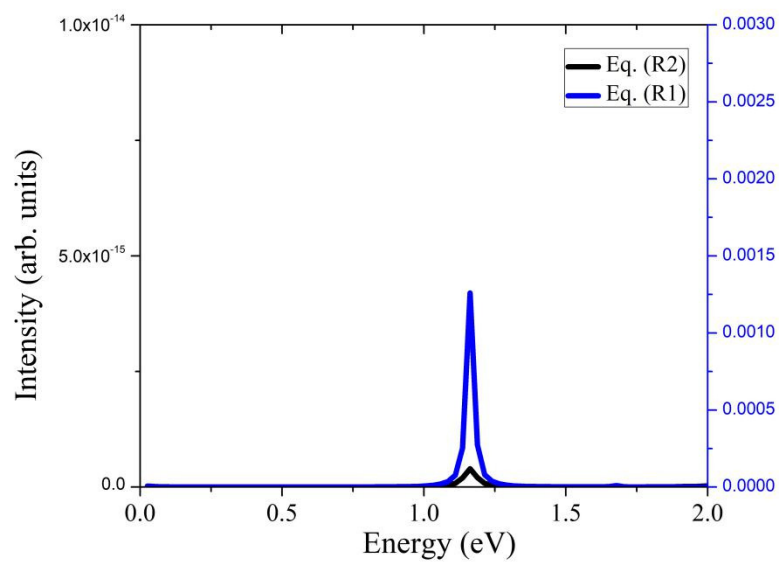


Fig. S1. Fourier transform spectra of the time-delay dependent wave-mixing harmonic signal (3,1). The blue and black lines are calculated through Eq. (S2) and (S3), respectively.

References

1. H. J. Werner, P. J. Knowles, G. Knizia, F. R. Manby, M. Schütz, “Molpro: a general-purpose quantum chemistry program package”, *WIREs Comput Mol Sci* **2**, 242 (2012).
2. I. Fdez, et al. “OpenMolcas: From Source Code to Insight”, *J. Chem. Theory Comput.* **15**, 5925 (2019).
3. S. C. Jiang, K. E. Dorfman, “Detecting electronic coherences by time-domain high-harmonic spectroscopy”, *Proc. Natl. Acad. Sci. United States Am.* **117**, 9776-9781 (2020).